Robust Adaptive Beamforming Method Based on Steering Vector Phase Correction and Covariance Matrix Reconstruction

Wolin Li, *Student Member, IEEE*, Xiaodong Qu, *Member, IEEE*, Xiaopeng Yang, *Senior Member, IEEE*, Bowen Han, *Student Member, IEEE*, Zhengyan Zhang, *Student Member, IEEE*, and Aly E. Fathy, *Life Fellow, IEEE*

***Abstract*— Steering vector (SV) mismatch caused by the DOA uncertainty in the source leads to a remarkable performance degradation for adaptive beamforming particularly in situation where the training data includes an unknown expected signal (ES) component. To mitigate this problem, a robust adaptive beamforming method based on SV phase correction and covariance matrix reconstruction is proposed in this letter. The first step is to correct the SV phase of the ES using the maximum *a posteriori* (MAP) estimation method. Next, the Gauss-Chebyshev quadrature is introduced to efficiently reconstruct the interference-plus-noise covariance matrix by integrating within the corrected azimuthal sector. The effectiveness and superiority of the proposed method in mitigating SV mismatch errors are confirmed by both numerical simulations and experimental results.**

***Index Terms*— Covariance matrix reconstruction, maximum *a posteriori*, phase correction, robust adaptive beamforming, steering vector mismatch.**

I. Introduction

ADAPTIVE beamforming is a crucial technology with broad applications in various fields such as astronomy, sonar, and communication [1], [2], [3]. However, conventional beamformers are limited to ideal scenarios. In practical application, the direction-of-arrival (DOA) of the expected signal (ES) is not accurately predictable, but a variable that incidents from an uncertain direction, which will cause a steering vector (SV) mismatch [4]. In this case, the ES component that is often inevitably included in the training data can significantly degrade the performance of the beamformer.

In response to these challenges, several robust adaptive beamforming (RAB) methods have been developed. The most widely used method was diagonal loading (DL) [5] but determining its optimal loading factor can be challenging. The worst-case performance optimization (WCPO) method [6] was proposed to address SV mismatch errors, whose upper bound is not easily obtained. Adaptive Bayesian beamforming (ABB) method [7] was developed to against source DOA uncertainty but only performs well under low signal-to-noise ratio (SNR). Several interference-plus-noise covariance matrix (INCM) reconstruction-based methods [8], [9], [10], [11], [12] have been proposed to mitigate the negative impact of ES component in the training data. However, these methods require accurate power spectrum and array structure information, which is sensitive to the SV mismatch errors [13], [14], and suffer from poor computational efficiency due to the high density of integral computations. Although each of these comparison methods has its advantages, they share the same significant drawback of output performance loss when there is a mismatch of the SV due to large DOA uncertainty.

To further enhance the efficiency and robustness of the beamformer, a new RAB method is developed in this letter. Initially, assume that the unknown ES randomly appears within *a priori* azimuthal sector, followed by the correction of the SV phase of ES using the maximum *a posteriori* (MAP) estimation. Subsequently, the INCM is reconstructed by integrating over the azimuthal sector where the estimated DOA of ES does not exists. Besides, the Gauss-Chebyshev quadrature is introduced as a replacement for integral operation to reduce computational complexity. Numerical simulation and experimental results will be presented to illustrate the effectiveness and robustness of the proposed method.

II. Signal Model and Background

Considering N-sensors uniform linear array (ULA) receives $Q+1$ far-field narrowband sources, including one ES and Q interferences. The array observation vector at time t is

$$\mathbf{x}(t) = \mathbf{a}_0 s_0(t) + \sum_{q=1}^{Q} \mathbf{a}_q s_q(t) + \mathbf{n}(t), \quad t = 1, 2, \cdots, K, \tag{1}$$

where $s_0(t)$, $s_q(t)$ and $\mathbf{a}_0$, $\mathbf{a}_q$ denote the waveform and the corresponding SV of ES and the q-th interference, respectively.

Manuscript received 27 July 2023; revised 28 September 2023; accepted 11 November 2023. Date of publication 23 November 2023; date of current version 9 January 2024. This work was supported by the National Natural Science Foundation of China under Grant 61860206012, Grant 62101042 and in part by the Natural Science Foundation of Chongqing under Grant cstc2020jcyj-msxmX0768 and Grant cstc2021jcyj-msxmX0339. This work was also supported by Beijing Institute of Technology Research Fund Program for Young Scholars. The associate editor coordinating the review of this letter and approving it for publication was H. Zhang. *(Corresponding author: Xiaodong Qu.)*

Wolin Li, Xiaodong Qu, Bowen Han, and Zhengyan Zhang are with the School of Information and Electronics, Beijing Institute of Technology, Beijing 100081, China, and also with the Key Laboratory of Electronic and Information Technology in Satellite Navigation, Ministry of Education, Beijing 100081, China (e-mail: 3120210739@bit.edu.cn; xdqu@bit.edu.cn; 3120185413@bit.edu.cn; 3120210782@bit.edu.cn).

Xiaopeng Yang is with the School of Information and Electronics, Beijing Institute of Technology, Beijing 100081, China, and also with the Yangtze Delta Region Academy, Beijing Institute of Technology, Jiaxing 314001, China (e-mail: xiaopengyang@bit.edu.cn).

Aly E. Fathy is with the Department of Electrical Engineering and Computer Science, University of Tennessee, Knoxville, TN 37996 USA (e-mail: fathy@ece.utk.edu).

Digital Object Identifier 10.1109/LCOMM.2023.3336217

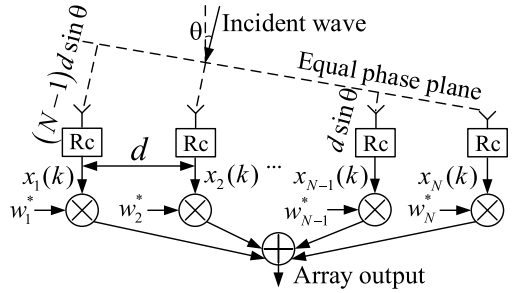

Fig. 1. Schematic of the ULA adaptive weighted output.

$\mathbf{n}(t)$ represents the Gaussian noise component with zero mean and σ_{n}^2 variance, and K is the number of snapshots. The form of SV when spaced half a wavelength can be expressed as

$$\mathbf{a}(\theta) = [1, e^{j\pi \sin\theta}, \cdots, e^{j(N-1)\pi \sin\theta}]^T. \tag{2}$$

The output of beamformer is represented as $\mathrm{y}(t) = \mathbf{w}^H \mathbf{x}(t)$ with the weight vector $\mathbf{w} = [w_1, w_2, \ldots, w_{\mathrm{N}}]^H$, which is clearly illustrated in the Fig. 1. The optimal weight vector, namely the MVDR beamformer [15], can be expressed as

$$\mathbf{w}_{\mathrm{opt}} = \mathbf{R}_{\mathrm{i+n}}^{-1}\mathbf{a}_0 / \left(\mathbf{a}_0^H \mathbf{R}_{\mathrm{i+n}}^{-1}\mathbf{a}_0\right), \tag{3}$$

where $\mathbf{R}_{\mathrm{i+n}} = \sum_{q=1}^{Q} \sigma_q^2 \mathbf{a}_q \mathbf{a}_q^H + \sigma_{\mathrm{n}}^2 \mathbf{I}$ denotes the theoretical INCM and $\mathbf{I}$ stands for identity matrix. In practical application, the $\mathbf{R}_{\mathrm{i+n}}$ and $\mathbf{a}_0$ in (3) are usually replaced by the sample covariance matrix (SCM) $\hat{\mathbf{R}}_{\mathrm{x}}$ and the nominal steering vector $\bar{\mathbf{a}}_0$, which significantly degrades the performance of beamformer, especially when SNR gets high.

III. Proposed Method Based on Steering Vector Phase Correction and Covariance Matrix Reconstruction

To mitigate the effect of SV mismatch errors caused by the DOA uncertainty and the existence of the ES component in SCM, an improved RAB method is proposed in this section.

A. Steering Vector Phase Correction

The SV mismatch errors is essentially the errors in the SV phase, which can be accurately corrected by using the MAP estimation method in this section. Firstly, assume that the ES is randomly incident from an uncertain angle θ within an azimuthal sector $\mathbf{\Phi}$ with *a priori* probability density function (pdf) $p(\theta)$. According to the Bayesian formula, the *a posteriori* pdf of $\theta_i \in \mathbf{\Phi}$ is given by

$$p(\theta|\mathbf{X}) = p(\theta)\, p(\mathbf{X}|\theta)/p(\mathbf{X}), \quad \theta \in \mathbf{\Phi}, \tag{4}$$

where $\mathbf{X} = [\mathbf{x}(t_1), \mathbf{x}(t_2), \cdots, \mathbf{x}(t_K)]$ stands for the received data matrix consisting of snapshots data vector $\mathbf{x}(t)$ taken at times $t_1, t_2, \cdots, t_K$. The likelihood function $p(\mathbf{X}|\theta)$ is the pdf of the data matrix $\mathbf{X}$ when given θ. Assume that the waveforms of the sources are zero-mean Gaussian random processes [16] and thus the likelihood function can be expressed as

$$p(\mathbf{X}|\theta) = \prod_{k=1}^{K} \frac{1}{\pi^N |\mathbf{R}_{\mathrm{x}}(\theta)|} \exp\left\{-\mathbf{x}^H(t_k)\, \mathbf{R}_{\mathrm{x}}^{-1}(\theta)\, \mathbf{x}(t_k)\right\}. \tag{5}$$

With the formula $\mathbf{R}_{\mathrm{x}} = \sigma_0^2 \mathbf{a}_0 \mathbf{a}_0^H + \mathbf{R}_{\mathrm{i+n}}$ and substituting (5) in (4), the *a posteriori* pdf is given by

$$p(\theta|\mathbf{X}) = c_1 p(\theta) \left(1 + \sigma_0^2 \beta(\theta)\right)^{-K} \cdot \exp\left\{\frac{\mathrm{K}\sigma_0^2 \mathbf{a}^H(\theta)\mathbf{R}_{\mathrm{i+n}}^{-1}(\theta)\hat{\mathbf{R}}_{\mathrm{x}}\mathbf{R}_{\mathrm{i+n}}^{-1}(\theta)\mathbf{a}(\theta)}{1+\sigma_0^2\beta(\theta)}\right\}, \tag{6}$$

where σ_0^2 represents the power of ES. c_1 is a constant independent of θ and $\hat{\mathbf{R}}_{\mathrm{x}} = \sum_{k=1}^{K} \mathbf{x}(t_k)\mathbf{x}^H(t_k)/K$ donates the SCM. $\beta(\theta) = \mathbf{a}^H(\theta)\mathbf{R}_{\mathrm{i+n}}^{-1}(\theta)\mathbf{a}(\theta)$ is a function of θ defined on $\mathbf{\Phi}$, where no interference component contained, i.e., $\mathbf{R}_{\mathrm{i+n}}(\theta) = \mathbf{R}_{\mathrm{n}} = \sigma_{\mathrm{n}}^2\mathbf{I}$, and hence the relationship $\beta(\theta) = \mathbf{a}^H(\theta)(\sigma_{\mathrm{n}}^2\mathbf{I})^{-1}\mathbf{a}(\theta) = N/\sigma_{\mathrm{n}}^2$ holds. Substitute it into (6), the *a posteriori* pdf can be simplified to

$$p(\theta|\mathbf{X}) = cp(\theta) \cdot \exp\left\{\gamma \mathbf{a}^H(\theta)\, \hat{\mathbf{R}}_{\mathrm{x}} \mathbf{a}(\theta)\right\}, \tag{7}$$

where c is a normalization constant. $\gamma = \mathrm{K}\sigma_0^2/(\sigma_{\mathrm{n}}^4 + N\sigma_0^2\sigma_{\mathrm{n}}^2)$ is another constant ,which only affects the magnitude of the probability and does not affect the estimation result, and can be set to any smaller number, such as 10^{-4}. With (7), an accurate estimate DOA of the ES can be obtained using the MAP estimation method

$$\hat{\theta}_0 = \arg\max_{\theta \in \mathbf{\Phi}} p(\theta|\mathbf{X}). \tag{8}$$

Therefore, the SV of ES can be accurately corrected as

$$\mathbf{a}(\hat{\theta}_0) = [1, e^{j\pi \sin\hat{\theta}_0}, \cdots, e^{j(N-1)\pi \sin\hat{\theta}_0}]^T. \tag{9}$$

Generally, by maximizing the utilization of the observed data and the *a priori* azimuthal sector of the ES component at a very low computational complexity, the proposed correction method is effective not only for the DOA uncertainty, but also for all other array error factors in the SV phase.

B. INCM Reconstruction

To further mitigate the performance deterioration due to the presence of the ES component in SCM, an improved and efficient method to reconstruction the INCM is proposed in this subsection.

Gu and Leshem proposed the most famous reconstruction method based on the Capon power spectrum integration [8], which is expressed as

$$\hat{\mathbf{R}}_{\mathrm{i+n}} = \int_{\bar{\mathbf{\Theta}}} \frac{\mathbf{a}(\theta)\, \mathbf{a}^H(\theta)}{\mathbf{a}^H(\theta)\, \hat{\mathbf{R}}_{\mathrm{x}}^{-1} \mathbf{a}(\theta)} d\theta, \tag{10}$$

where $\bar{\mathbf{\Theta}}$ is the complement of the *a priori* azimuthal sector of the ES in the whole spatial domain [8]. However, the performance of this method is highly dependent on the accuracy of the *a priori* azimuthal sector $\mathbf{\Theta}$. To improve it, the $\hat{\theta}_0$ estimated in (8) is used to correct the integral interval as follows

$$\bar{\mathbf{\Theta}} = [-90^\circ, \hat{\theta}_0 - \theta_{mb}] \cup [\hat{\theta}_0 + \theta_{mb}, 90^\circ], \tag{11}$$

where θ_{mb} stands for the width of the integral interval, which usually can be set to $\theta_{mb} = 101.4/N(^\circ)$ for ULA spaced half a wavelength [1].

In addition, the integral operation in (10) is computationally intensive, limiting the algorithm's applicability in scenarios

where fast processing times are critical. To further improve the efficiency, Gauss-Chebyshev quadrature [17] is introduced to quickly calculate the reconstructed INCM, which can be expressed in detail as

$$\int_a^b \frac{f(x)}{\sqrt{1-x^2}}dx \approx \frac{b-a}{2}\sum_{k=1}^{n} w_k \sqrt{1-y_k^2}\frac{f(x_k)}{\sqrt{1-x_k^2}}, \quad (12)$$

where $x_k = (b-a)y_k/2 + (b+a)/2$, the weight $w_k = \pi/n$, and the Chebyshev nodes $y_k = \cos((2k-1)\pi/(2n))$ are the roots of the Chebyshev polynomials of the first kind for the given positive integer n. Use the integration by substitution, i.e. let $x = \sin\theta$, thus converting the integrand in (10) into the form $f(x)/\sqrt{1-x^2}$, where $f(x) = \mathbf{a}(x)\mathbf{a}^H(x)\Big/(\mathbf{a}^H(x)\hat{\mathbf{R}}^{-1}\mathbf{a}(x))$ with $\mathbf{a}(x) = [1, e^{j\pi x}, \cdots, e^{j(N-1)\pi x}]^T$ of ULA spaced half a wavelength.

Moreover, it's found that the proposed method performs better when the DL technology [5] is used appropriately to preprocess the SCM, i.e., we substitute

$$\hat{\mathbf{R}}_{\mathrm{x}} = \sum_{k=1}^{K} \mathbf{x}(t_k)\mathbf{x}^H(t_k)/K + \sigma_{\mathrm{DL}}^2\mathbf{I} \quad (13)$$

for the SCM in (7) and (10), where σ_{DL}^2 is the loading factor, usually set to 10 times the noise power.

The effectiveness of the proposed method in improving the accuracy of the reconstructed INCM and the performance of beamformer under DOA uncertainty will be demonstrated through simulations and experimental results in Section IV, where the corrected integral interval plays a significant role.

C. Adaptive Weight Vector Calculation

Based on the corrected SV in (9) and the reconstructed INCM in (10), the adaptive weight vector is calculated by

$$\mathbf{w} = \hat{\mathbf{R}}_{\mathrm{i+n}}^{-1}\mathbf{a}\left(\hat{\theta}_0\right)\Big/\left(\mathbf{a}^H\left(\hat{\theta}_0\right)\hat{\mathbf{R}}_{\mathrm{i+n}}^{-1}\mathbf{a}\left(\hat{\theta}_0\right)\right). \quad (14)$$

Therefore, the proposed method can overcome the mismatch errors caused by the DOA uncertainty and effectively improve the robustness of the beamformer. The proposed method is summarized in Algorithm 1.

The computational complexity of the SV correction, the INCM reconstruction and the weight vector calculation are about $\mathcal{O}(N^2)$, $\mathcal{O}(nN^2)$, $\mathcal{O}(N^3)$, respectively, where n is the order of Gauss-Chebyshev quadrature, and it is enough to set it to 60. While the corresponding computational complexity of REB is $\mathcal{O}(N^{3.5})$, $\mathcal{O}(SN^2)$ and $\mathcal{O}(N^3)$, where S is the number of sampling points and typically $S \gg N$.

It's worth noting that when the number of sensors N is large, the Toeplitz structure [18], [19] of INCM can be used to further reduce the complexity to $\mathcal{O}(nN)$ by using the formula $(\tilde{\mathbf{R}}_{\mathrm{i+n}})_{pq} = \int_{\tilde{\mathbf{\Theta}}} \exp(j(p+q-2)\pi\sin\theta)\Big/(\mathbf{a}^H(\theta)\hat{\mathbf{R}}_{\mathrm{x}}^{-1}\mathbf{a}(\theta))d\theta$ we derived, where p and q are the number of rows and columns of the INCM, respectively.

IV. Performance Analysis

In this section, we conducted simulations and experiments to assess the effectiveness of the proposed method, and the results are presented in the following.

Algorithm 1 Correction and Reconstruction Method

1) Input: $\mathbf{X}, \mathbf{\Phi}, p(\theta)$;

2) Initialization: Set $K = 50$, $\sigma_{DL}^2 = 10\hat{\sigma}_{\mathrm{n}}^2$, $\gamma = 10^{-4}$, $n = 60$;

3) Calculate the SCM $\hat{\mathbf{R}}_{\mathrm{x}}$ with $\mathbf{X}$ using (13);

4) Estimate the $\hat{\theta}_0$ and correct the SV by (7), (8) and (9);

5) Reconstruct the INCM with $\hat{\theta}_0$ from(10), (11) and (12);

6) Get the adaptive weight $\mathbf{w}$ according to (14).

A. Numerical Simulations

In the simulations, considering a ULA with $N = 16$ sensors spaced half a wavelength, and the noise is seen as Gaussian additive noise with zero-mean and unity variance. The look direction of the array is defined as $0°$. Three far-field narrowband sources are set in all simulations, including one ES with the uncertain DOA uniformly distributed in the *a priori* azimuthal sector $\mathbf{\Phi}$, i.e., the *a priori* pdf $p(\theta)$ is a constant, and two interferences with zero-mean Gaussian random waveforms arriving from $\theta_1 = -30°$ and $\theta_2 = 60°$, respectively. In all simulations, the interference-to-noise ratio (INR) is set to 20dB and the results are based on 1000 Monte-Carlo trials. The other parameters are listed in Algorithm 1. The simulation results are compared with four commonly used RAB methods, including the DL method in [5] with loading factor $\sigma_{\mathrm{DL}}^2 = 10\hat{\sigma}_{\mathrm{n}}^2$, the WCPO method in [6] with the upper bounding $\varepsilon = 0.2N$, the ABB method in [7], and the REB method in [8] with the eliminated angular sector $[-\theta_{mb}, \theta_{mb}]$.

First of all, to test the convergence speed of the proposed method with the increase of the number of snapshots (K), Fig.2(a) shows the curves of the output signal-to-interference-plus-noise ratio (SINR) versus $K$when SNR=20dB and $\mathbf{\Phi}$ is set to $[-8°, 8°]$. The output SINR is calculated as follows

$$\mathrm{SINR} = \sigma_0^2\left|\mathbf{w}^H\mathbf{a}_0\right|^2\Big/\left(\mathbf{w}^H\mathbf{R}_{\mathrm{i+n}}\mathbf{w}\right). \quad (15)$$

It's clear from Fig.2(a) that the proposed method converges even though the K value is extremely small and remains very close to the stable output SINR of the theoretical optimal value. Conversely, all comparison methods converge very slowly with a large performance degradation.

The normalized beampatterns are drawn in Fig.2(b) when SNR=20dB, $\mathbf{\Phi} = [-8°, 8°]$ and K fixed at 50, which illustrate that both the DL and ABB algorithm fail to efficiently capture the ES, but inadvertently form a deep null in the direction of ES. However, both the REB and the proposed method adaptively form a high-gain mainlobe in the unpredictable direction of ES, while the proposed method is more accurate than the REB, thus achieving effective signal reception.

To further verify the performance of proposed method, the output SINR versus input SNR curve with K fixed at 50 when $\mathbf{\Phi} = [-5°, 5°]$ and $\mathbf{\Phi} = [-8°, 8°]$ is shown in Fig.2(c) and (d), respectively. The results show that the output

TABLE I
EXPERIMENTAL PERFORMANCE IMPROVEMENTS

Method	Output SINR (dB)	Improvements (dB)
DL	4.9dB	12.0dB
WCPO	4.1dB	11.2dB
ABB	6.2dB	13.3dB
REB	7.5dB	14.6dB
Proposed	9.2dB	16.3dB

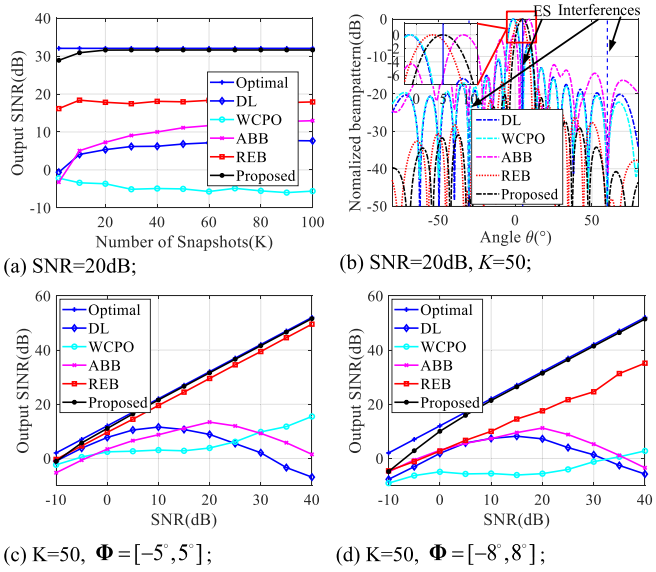

(a) SNR=20dB; (b) SNR=20dB, K=50;

(c) K=50, $\mathbf{\Phi}=[-5^\circ,5^\circ]$; (d) K=50, $\mathbf{\Phi}=[-8^\circ,8^\circ]$;

Fig. 2. Numerical simulation results; (a) Output SINR versus number of snapshots; (b) Adaptive Beampatterns; (c)(d) Output SINR versus SNR.

performance of DL and ABB deteriorates severely with the increase of SNR, while the curve of WCPO method maintains an upward trend, but still far from the theoretical optimal curve and even worse than all other comparison methods with low SNR, which is attributed to the direct use of SCM containing the ES component. The REB method achieves a great performance improvement through the reconstruction technique, but as shown in Fig.2(d), when the *a priori* azimuthal sector is large, i.e., the *a priori* angular information is not accurate enough, its performance loss is too large to be acceptable. On the contrary, the proposed method can stably maintain very good performance that is considerably close to the theoretical optimal value in all case. It confirms that the proposed method accurately corrects the SV and successfully solves the mismatch errors caused by DOA uncertainty through a low-complexity estimation and reconstruction method.

B. Experimental Results

In this section, we conducted experiments by a 16-sensors and 4-channels phased array radar working at 16GHz, and the experimental scenario is shown in Fig. 3(a). In the experiments, we set up three far-field narrowband signal sources, including one ES and two sidelobe interferences. The look direction of the radar is defined as 0°, which is where we want the ES to incident, but the actual angle will be biased due to the inevitable error of manual operation. That is, the actual ES is not incident from the look direction as we expect,

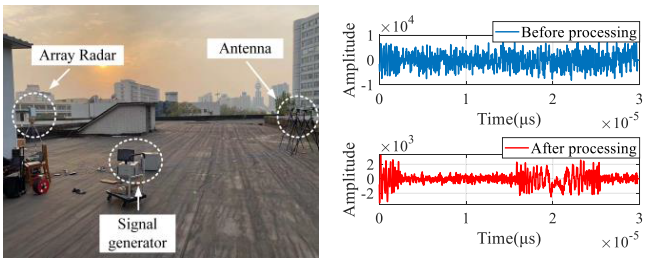

(a) Experimental scenario; (b) Time domain waveform;

Fig. 3. Experimental scenario and time domain waveform before and after processing by the proposed method.

but from an uncertain range. We limit this range to $[-5^\circ, 5^\circ]$ when setting up the experimental antenna.

The time domain waveforms of collected data before and after processing using the proposed method are shown in Fig.3(b), which illustrate that the ES is completely masked by strong interferences and noise before processing, and therefore cannot be effectively detected. The proposed method can effectively suppress interferences and noise, so the waveform of ES can be clearly displayed and distinguished after processing as shown in Fig.3(b). The results of the output SINR performance improvement of all comparison methods is shown in Table I. The input SNR and INR of the collected data are about 8.5dB and 15.6dB, respectively. It means that the input SINR is approximately -7.1dB. Therefore, the difference between the output SINR and the input SINR is the performance improvement before and after the algorithm processing. It can be found that the proposed method keeps an improvement advantage of about 2dB in the processing of experimental data, which is a relatively large technological progress considering the complex electromagnetic interference situation in the actual experimental scenario.

V. CONCLUSION

In this letter, a robust adaptive beamforming method has been proposed to enhance the robustness against SV mismatch errors dominated by the source's DOA uncertainty. In the proposed method, the accurate SV phase of ES is corrected by using the MAP estimation with a random uniform distribution within *a priori* azimuthal sector based on Bayesian hypothesis. Subsequently, the INCM is reconstructed by integrating over the azimuthal sector where removed the estimated DOA of ES using the efficient Gauss-Chebyshev quadrature. Therefore, the proposed method can overcome the mismatch errors essentially and the robustness of adaptive beamforming can be improved significantly. The numerical simulations and experimental results have demonstrated that the proposed method can achieve a better performance in the presence of source's DOA uncertainty.

REFERENCES

[1] C. Pell, "Phased-array radars," *IEE Rev.*, vol. 34, no. 9, pp. 363–367, Oct. 1988, doi: 10.1049/ir:19880149.
[2] H. L. Van Trees, *Optimum Array Processing—Part IV of Detection, Estimation, and Modulation Theory*. New York, NY, USA: Wiley, 2002, pp. 6–12.

[3] J. Yang, Y. Tu, J. Lu, and Z. Yang, "Robust adaptive beamforming based on subspace decomposition, steering vector estimation and correction," *IEEE Sensors J.*, vol. 22, no. 12, pp. 12260–12268, Jun. 2022, doi: 10.1109/JSEN.2022.3174848.

[4] C.-C. Lee and J.-H. Lee, "Eigenspace-based adaptive array beamforming with robust capabilities," *IEEE Trans. Antennas Propag.*, vol. 45, no. 12, pp. 1711–1716, Dec. 1997, doi: 10.1109/8.650188.

[5] B. D. Carlson, "Covariance matrix estimation errors and diagonal loading in adaptive arrays," *IEEE Trans. Aerosp. Electron. Syst.*, vol. 24, no. 4, pp. 397–401, Jul. 1988, doi: 10.1109/7.7181.

[6] S. A. Vorobyov, A. B. Gershman, and Z.-Q. Luo, "Robust adaptive beamforming using worst-case performance optimization: A solution to the signal mismatch problem," *IEEE Trans. Signal Process.*, vol. 51, no. 2, pp. 313–324, Feb. 2003, doi: 10.1109/tsp.2002.806865.

[7] K. L. Bell, Y. Ephraim, and H. L. Van Trees, "A Bayesian approach to robust adaptive beamforming," *IEEE Trans. Signal Process.*, vol. 48, no. 2, pp. 386–398, Feb. 2000, doi: 10.1109/78.823966.

[8] Y. Gu and A. Leshem, "Robust adaptive beamforming based on interference covariance matrix reconstruction and steering vector estimation," *IEEE Trans. Signal Process.*, vol. 60, no. 7, pp. 3881–3885, Jul. 2012, doi: 10.1109/TSP.2012.2194289.

[9] Y. Gu, N. A. Goodman, S. Hong, and Y. Li, "Robust adaptive beamforming based on interference covariance matrix sparse reconstruction," *Signal Process.*, vol. 96, pp. 375–381, Mar. 2014, doi: 10.1016/j.sigpro.2013.10.009.

[10] L. Huang, J. Zhang, X. Xu, and Z. Ye, "Robust adaptive beamforming with a novel interference-plus-noise covariance matrix reconstruction method," *IEEE Trans. Signal Process.*, vol. 63, no. 7, pp. 1643–1650, Apr. 2015, doi: 10.1109/TSP.2015.2396002.

[11] Z. Zhang, W. Liu, W. Leng, A. Wang, and H. Shi, "Interference-plus-noise covariance matrix reconstruction via spatial power spectrum sampling for robust adaptive beamforming," *IEEE Signal Process. Lett.*, vol. 23, no. 1, pp. 121–125, Jan. 2016, doi: 10.1109/LSP.2015.2504954.

[12] X. Yuan and L. Gan, "Robust adaptive beamforming via a novel subspace method for interference covariance matrix reconstruction," *Signal Process.*, vol. 130, pp. 233–242, Jan. 2017, doi: 10.1016/j.sigpro.2016.07.008.

[13] H. Yang, P. Wang, and Z. Ye, "Robust adaptive beamforming via covariance matrix reconstruction under colored noise," *IEEE Signal Process. Lett.*, vol. 28, pp. 1759–1763, 2021, doi: 10.1109/LSP.2021.3105930.

[14] P. Chen, Y. Yang, Y. Wang, and Y. Ma, "Adaptive beamforming with sensor position errors using covariance matrix construction based on subspace bases transition," *IEEE Signal Process. Lett.*, vol. 26, no. 1, pp. 19–23, Jan. 2019, doi: 10.1109/LSP.2018.2878948.

[15] J. Li and P. Stocia, *Robust Adaptive Beamforming*. New York, NY, USA: Wiley, 2005, pp. 14–18.

[16] Y. Ephraim, "A Bayesian estimation approach for speech enhancement using hidden Markov models," *IEEE Trans. Signal Process.*, vol. 40, no. 4, pp. 725–735, Apr. 1992, doi: 10.1109/78.127947.

[17] M. Abramowitz and I. A. Stegun, "Numerical interpolation, differentiation and integration," in *Handbook of Mathematical Functions: With Formulas, Graphs, and Mathematical Tables*. New York, NY, USA: Dover, 1964, pp. 887–889.

[18] Y.-M. Chen, J.-H. Lee, C.-C. Yeh, and J. Mar, "Bearing estimation without calibration for randomly perturbed arrays," *IEEE Trans. Signal Process.*, vol. 39, no. 1, pp. 194–197, Jan. 1991, doi: 10.1109/78.80780.

[19] D. A. Linebarger, "Redundancy averaging with large arrays," *IEEE Trans. Signal Process.*, vol. 41, no. 4, pp. 1707–1710, Apr. 1993, doi: 10.1109/78.212750.